05,07

Weak ferrimagnets of the $YFe_{1-x}Cr_xO_3$ type: negative magnetization and spin reorientation

© E.V. Vasinovich [1], A.S. Moskvin [1,2]

[1] Ural Federal University,
Yekaterinburg, Russia
[2] M.N. Mikheev Institute of Metal Physics, Ural Branch, Russian Academy of Sciences,
Yekaterinburg, Russia

E-mail: evgeny.vasinovich@urfu.ru

In this work, we present an analysis of magnetic properties of weak ferrimagnets of the $YFe_{1-x}Cr_xO_3$ type. Taking into account the main spin interactions — isotropic Heisenberg superexchange, antisymmetric Dzyaloshinskii–Moriya exchange, single-ion spin anisotropy — calculations of the free energy, concentration and temperature dependences of magnetization were carried out within a framework of a molecular field model. In particular, the model demonstrates the phenomena of temperature compensation and negative magnetization, as well as spin reorientation. The compensation temperature reaches room temperature $T = 300\,K$ in a composition with $x \approx 0.45$. The existence of magnetic structures of the G_{xyz} type with the spatial orientation of the Neel vector is predicted.

1. Introduction

Rare-earth orthoferrites-orthochromites of the type $RFe_{1-x}Cr_xO_3$ (R = Nd, Gd, Dy, Y, Lu) have been the subject of intensive fundamental theoretical and experimental studies in the second half of the 20th century owing to the combination of its unique magnetic, magneto-optical, magneto-elastic and magnetic resonance properties, primarily weak ferro- and antiferromagnetism, spin-reorientation (SR) transitions, the phenomenon of magnetic moment compensation and negative magnetization. Moreover, the studies of mixed orthoferrite-orthochromite $YFe_{1-x}Cr_xO_3$ conducted more than 50 years ago led to the theoretical prediction and experimental discovery of a new phenomenon — a weak ferrimagnetism resulting from the competition of signs of the Dzyaloshinskii vector [2].

A new surge of interest in these systems already in the 21st century (see, for example, [3–12]) is associated with the prospects for practical application of the phenomenon of temperature compensation of the magnetic moment and the associated effects of „negative" magnetization and exchange bias to create various multifunctional spintronics devices. However, we encounter both ambiguity of experimental data and ambiguity in their interpretation in most „new" works devoted to the study of weak ferrimagnets of the type $YFe_{1-x}Cr_xO_3$.

In particular, with respect to the Neel temperature T_N, it is only known that it decreases monotonously with the change of the composition from $YFeO_3$ to $YCrO_3$ [2,10], but there is no consensus with respect to the exact value of T_N and, for example, values T_N from $210-250\,K$ [2–7] and up to $T_N = 340-360\,K$ [2] are reported for the composition $YFe_{0.5}Cr_{0.5}O_3$, which is apparently attributable to the peculiarities of polycrystalline samples and small magnitudes of magnetization. There are even less data on the compensation temperature T_{comp} and they are also contradictory, for example, both the temperature of $T_{comp} = 175\,K$ [11] and $T_{comp} = 248\,K$ is reported for the system of $YFe_{0.5}Cr_{0.5}O_3$ [3]. There are also problems with choosing a computational scheme for approximating the molecular field and misinterpreting the nature of the phenomenon of magnetic moment compensation, for example, as a result of competition between single-ion spin anisotropy and the Dzyaloshinskii–Moriya interaction. In contrast to spin reorientation in weak ferromagnets with a magnetic rare-earth ion (see, for example, [1,13,14]), the SR transition in weak ferrimagnets $RFe_{1-x}Cr_xO_3$ with a non-magnetic R ion (La, Y, Lu) has also not yet received an adequate description.

This paper developing the model concepts laid down by A.M. Kadomtseva and colleagues [2] presents a sequential molecular field analysis of the magnetic properties of weak ferrimagnets of the type $YFe_{1-x}Cr_xO_3$.

2. Model

The mixed systems of $YFe_{1-x}Cr_xO_3$, like the „parent" orthoferrites and orthochromites, are orthorhombic perovskites with the spatial group $Pbnm$. There are 4 magnetic

$3d$-ions per lattice cell (see Figure 1), for which the following classical basis vectors can be introduced:

$$4S\mathbf{F} = \mathbf{S}^{(1)} + \mathbf{S}^{(2)} + \mathbf{S}^{(3)} + \mathbf{S}^{(4)},$$

$$4S\mathbf{G} = \mathbf{S}^{(1)} - \mathbf{S}^{(2)} + \mathbf{S}^{(3)} - \mathbf{S}^{(4)},$$

$$4S\mathbf{C} = \mathbf{S}^{(1)} + \mathbf{S}^{(2)} - \mathbf{S}^{(3)} - \mathbf{S}^{(4)},$$

$$4S\mathbf{A} = \mathbf{S}^{(1)} - \mathbf{S}^{(2)} - \mathbf{S}^{(3)} + \mathbf{S}^{(4)}. \quad (1)$$

Here the vector $\mathbf{G}$ describes the main antiferromagnetic component of the magnetic structure (the Neel vector), $\mathbf{F}$ — the vector of weak ferromagnetism (overt canting of sublattices), weak antiferromagnetic components $\mathbf{C}$ and $\mathbf{A}$ describe the canting of magnetic sublattices without the formation of a total magnetic moment (hidden canting of sublattices). „Allowed" spin configurations for $3d$-sublattices compatible with the antiferromagnetic sign of the main isotropic superexchange are denoted as $\Gamma_1\,(A_x, G_y, C_z)$, $\Gamma_2\,(F_x, C_y, G_z)$, $\Gamma_4\,(G_x, A_y, F_z)$, where the only non-zero components of the basis vectors appear in parentheses. A transition from one configuration to another is possible in the process of spin reorientation.

Let us present the spin-Hamiltonian of a weak ferrimagnet in the simplest form, taking into account only the contributions of the isotropic exchange interaction, the antisymmetric Dzyaloshinskii–Moriya exchange (DM) and a simplified form of the second-order single-ion spin anisotropy

$$\hat{H} = \hat{H}_{ex} + \hat{H}_{DM} + \hat{H}_{SIA}^{(2)},$$

$$\hat{H}_{ex} = \frac{1}{2}\Sigma_{\langle mn\rangle} I_{mn}(\hat{\mathbf{S}}_m \cdot \hat{\mathbf{S}}_n),$$

$$\hat{H}_{DM} = \frac{1}{2}\Sigma_{\langle mn\rangle} \mathbf{d}_{mn} \cdot [\hat{\mathbf{S}}_m \times \hat{\mathbf{S}}_n],$$

$$\hat{H}_{SIA}^{(2)} = D\left(\hat{S}_z^2 - \frac{1}{3}S(S+1)\right), \quad (2)$$

where summation occurs over the nearest neighbors, I_{mn} – exchange integral, $\mathbf{d}_{mn}$ — Dzyaloshinskii vector, D — anisotropy constant, which, generally speaking, differs for ions Fe^{3+} and Cr^{3+} (for simplicity of writing in $\hat{H}_{SIA}^{(2)}$, summation by lattice sites is omitted).

Figure 1 shows the structure of superexchange bonds in the model. The ions at position 1 interact with four nearest neighbors in the a-plane and two ions along the c-axis. The cation-anion distances and the superexchange bond angles for the nearest neighbors slightly differ, so below we assume the equality of the superexchange integrals $I_{ab} = I_c = I$ and the modules of the Dzyaloshinskii vectors $d_{ab} = d_c = d$, although the vectors themselves are directed in different directions.

Back in 1970, A.S. Moskvin obtained a microscopic expression of the relation of the Dzyaloshinskii vector with the geometry of the superexchange bond cation-anion-cation [15] (see also Ref. [16,17] and later review
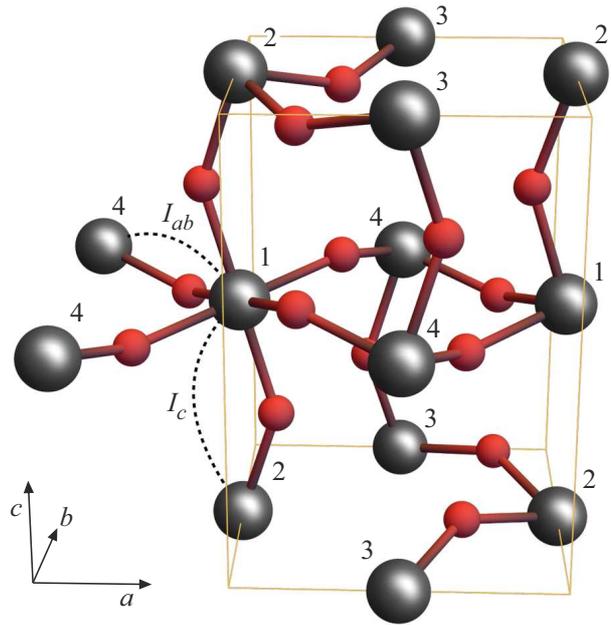
Figure 1. The structure of superexchange bonds; large balls — Fe^{3+}, Cr^{3+} ions, small — O^{2-}; $1, 2, 3, 4$ — magnetic ions in four non-equivalent positions.

Table 1. Components x, y, z of structural factors $[\mathbf{r}_m \times \mathbf{r}_n]$ calculated using the neutron diffraction data [11] for $YFe_{0.5}Cr_{0.5}O_3$

	x	y	z
$[\mathbf{r}_2 \times \mathbf{r}_1]$	0.216	0.562	0
$[\mathbf{r}_4 \times \mathbf{r}_1]$	± 0.303	0.287	0.397

articles [18–22]):

$$\mathbf{d}_{mn} = d_{mn}(\theta)[\mathbf{r}_m \times \mathbf{r}_n], \quad (3)$$

where $\mathbf{r}_{m,n}$ — unit vectors along the bonds O^{2-} — Fe^{3+}, or $O^{2-} - Cr^{3+}$, θ — the angle of the superexchange bond. The structural factors determining the orientation of the Dzyaloshinskii vectors in orthoferrites-orthochromites of the type $YFe_{1-x}Cr_xO_3$ are given in Table 1.

The simple formula (3) allows determining a direct relationship of magnetic non-collinearity (overt and hidden canting of sublattices) in weak ferromagnets with a crystal structure [16–22]. The most important result of the microscopic theory of antisymmetric exchange [17–22] was not so much an estimate of the numerical value as the prediction of the sign of the Dzyaloshinskii vector, in particular, of different signs in pairs $Fe^{3+} - Fe^{3+}$, $Cr^{3+} - Cr^{3+}$ on the one hand and pairs $Fe^{3+} - Cr^{3+}$, $Cr^{3+} - Fe^{3+}$ on the other hand, which played a fundamental role in prediction and experimental discovery of a new type of magnetic ordering — weak ferrimagnetism [2,17–22].

Table 2. Coupling of spin components on different sublattices in phases Γ_1, Γ_2 and Γ_4

Γ_1 (A_x, G_y, C_z)	Γ_2 (F_x, C_y, G_z)	Γ_4 (G_x, A_y, F_z)
$S_x^{(1)} = -S_x^{(2)} = -S_x^{(3)} = S_x^{(4)}$	$S_x^{(1)} = S_x^{(2)} = S_x^{(3)} = S_x^{(4)}$	$S_x^{(1)} = -S_x^{(2)} = S_x^{(3)} = -S_x^{(4)}$
$S_y^{(1)} = -S_y^{(2)} = S_y^{(3)} = -S_y^{(4)}$	$S_y^{(1)} = S_y^{(2)} = -S_y^{(3)} = -S_y^{(4)}$	$S_y^{(1)} = -S_y^{(2)} = -S_y^{(3)} = S_y^{(4)}$
$S_z^{(1)} = S_z^{(2)} = -S_z^{(3)} = -S_z^{(4)}$	$S_z^{(1)} = -S_z^{(2)} = S_z^{(3)} = -S_z^{(4)}$	$S_z^{(1)} = S_z^{(2)} = S_z^{(3)} = S_z^{(4)}$

3. Mean field approximation

The bilinear part of the Hamilton operator (2) is represented as follows in the simplest model of weak ferrimagnets of the type $R\mathrm{Fe}_{1-x}\mathrm{Cr}_x\mathrm{O}_3$ $(R = \mathrm{La, Y, Lu})$, assuming a single magnetic ordering in Fe-Cr-subsystem with molecular fields common to all ions $\mathrm{Fe}^{3+}(\mathrm{Cr}^{3+})$

$$\hat{H}_{ex} + \hat{H}_{DM} = \Sigma_n(\mathbf{h}_n \cdot \hat{\mathbf{S}}_n) - \frac{1}{2}\Sigma_n(\mathbf{h}_n \cdot \langle \mathbf{S}_n \rangle), \qquad (4)$$

where we have the following equation for the molecular field $\mathbf{h}_n$ at the node n, taking into account the leading contributions of isotropic exchange and the Dzyaloshinskii–Moriya interaction

$$\mathbf{h}_n = \Sigma_m(I_{mn}\langle \mathbf{S}_m \rangle + [\mathbf{d}_{mn} \times \langle \mathbf{S}_m \rangle]), \qquad (5)$$

here $\langle \mathbf{S}_m \rangle$ — thermodynamic average of the spin of an arbitrary ion (Fe^{3+} or Cr^{3+})

$$\langle \mathbf{S}_m \rangle = -\frac{\mathbf{h}_m}{h_m} SB_S\left(\frac{Sh_m}{k_B T}\right), \qquad (6)$$

B_S — Brillouin function, $h_m = |\mathbf{h}_m|$.

Obviously, we are forced to introduce a number of additional assumptions and approximations for solving molecular field equations (6) for weak ferrimagnets of the type $\mathrm{YFe}_{1-x}\mathrm{Cr}_x\mathrm{O}_3$ unlike the homogeneous parent systems of YFeO_3 and YCrO_3:

1) Fe^{3+} and Cr^{3+} ions are equally likely to fill the lattice nodes;

2) the spin-Hamiltonian parameters do not depend on either the local configuration or the concentration of Fe^{3+} and Cr^{3+} ions;

3) the long-range crystalline and magnetic (spin) orders are preserved, that is, the classification of possible magnetic structures ($\Gamma_{1,2,4}$) and the corresponding ratios between the average values of spin moments in positions 1, 2, 3 and 4 are preserved (see Table 2), which allows considering the equations of the molecular field for only one position of $3d$-ions.

So, we get

$$\begin{aligned}\mathbf{h}_{\mathrm{Fe}} = P_{\mathrm{Fe}}(x)\langle 4I_{\mathrm{FeFe}}\hat{\mathbf{S}}_{\mathrm{Fe}}^{(4)} + 2I_{\mathrm{FeFe}}\hat{\mathbf{S}}_{\mathrm{Fe}}^{(2)} \\ + 4[\mathbf{d}_{\mathrm{FeFe}}^{(41)} \times \hat{\mathbf{S}}_{\mathrm{Fe}}^{(4)}] + 2[\mathbf{d}_{\mathrm{FeFe}}^{(21)} \times \hat{\mathbf{S}}_{\mathrm{Fe}}^{(2)}]\rangle \\ + P_{\mathrm{Cr}}(x)\langle 4I_{\mathrm{FeCr}}\hat{\mathbf{S}}_{\mathrm{Cr}}^{(4)} + 2I_{\mathrm{FeCr}}\hat{\mathbf{S}}_{\mathrm{Cr}}^{(2)} \\ + 4[\mathbf{d}_{\mathrm{FeCr}}^{(41)} \times \hat{\mathbf{S}}_{\mathrm{Cr}}^{(4)}] + 2[\mathbf{d}_{\mathrm{FeCr}}^{(21)} \times \hat{\mathbf{S}}_{\mathrm{Cr}}^{(2)}]\rangle, \qquad (7)\end{aligned}$$

for the molecular field $\mathbf{h}_{\mathrm{Fe}}$ at position 1, where $P_{\mathrm{Fe}}(x) = 1 - x$, $P_{\mathrm{Cr}}(x) = x$ — concentrations of ions Fe^{3+} and Cr^{3+} accordingly, the brackets $\langle \ldots \rangle$ mean the thermodynamic average, the components of the vectors $\mathbf{S}^{(2)}$ and $\mathbf{S}^{(4)}$ are expressed in terms of $\mathbf{S}^{(1)}$ in accordance with Table 2. The field $\mathbf{h}_{Cr}$ has the same shape, but with the substitution of $\mathrm{Fe} \leftrightarrow \mathrm{Cr}$ in the right part. It should be noted that the nonequivalent contributions of bonds $1-2$ and $1-4$ are highlighted in (7), which is especially important given the different orientation of the Dzyaloshinskii vectors for these bonds. Therefore, the system (6), in fact, consists of two (for ion Fe^{3+} and ion Cr^{3+}) vector self-consistent equations.

4. Results

The system (6) was solved numerically for the following exchange parameters: $I_{FeFe} = 36.6$ K and $I_{CrCr} = 18.7$ K calculated using the Neel temperatures of orthoferrite YFeO_3, $T_N(0) = 640$ K [23], and orthochromite YCrO_3, $T_N(1) = 140$ K [24]. The exchange integrals between the ions Fe-Cr and Cr-Fe were assumed to be the same: $I_{FeCr} = I_{CrFe} = 13.4 \pm 0.4$ K according to the data from Ref. [25]. The scalar parameters of the antisymmetric Dzyaloshinskii–Moriya exchange $d_{FeFe} = 2.0$ K and $d_{CrCr} = 1.7$ K were selected based on saturation magnetization data $M = 1.5$ emu/g in „parent" YFeO_3 and YCrO_3 [2]. In accordance with the predictions of microscopic theory [17–22], the parameter $d_{FeCr} = d_{CrFe}$ should have a sign opposite to the sign of the parameters d_{FeFe} and d_{CrCr}, its value $d_{FeCr} = d_{CrFe} = -2.5$ K it was chosen to match the calculated compensation temperature with the observed temperature $T_{comp} \approx 225$ K for single crystal samples $\mathrm{YFe}_{1-x}\mathrm{Cr}_x\mathrm{O}_3$ at $x = 0.38$ [26].

Figure 2 shows the results of calculation of the temperature dependences of the magnetization of a weak ferrimagnet $\mathrm{YFe}_{1-x}\mathrm{Cr}_x\mathrm{O}_3$ at some concentrations from $x = 0$ to $x = 1$ with the assumption of preservation of the magnetic configuration Γ_4. The region where $M < 0$ corresponds to negative magnetization.

It should be noted that the condition of preservation of the magnetic configuration is a critical constraint of the model: despite good qualitative agreement with the experiment, the saturation magnetization of single crystal samples with $x = 0.38$, 0.5, 0.65 is significantly, in two-three times less than the predictions of the theory, which in the light of
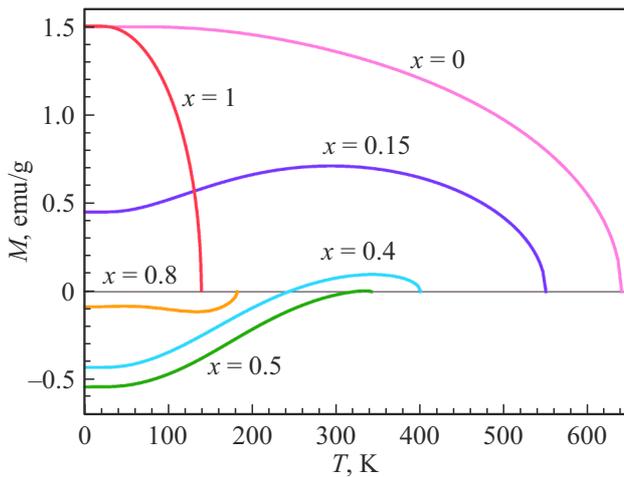
Figure 2. Temperature dependence of magnetization of $YFe_{1-x}Cr_xO_3$ at different chromium concentrations x.
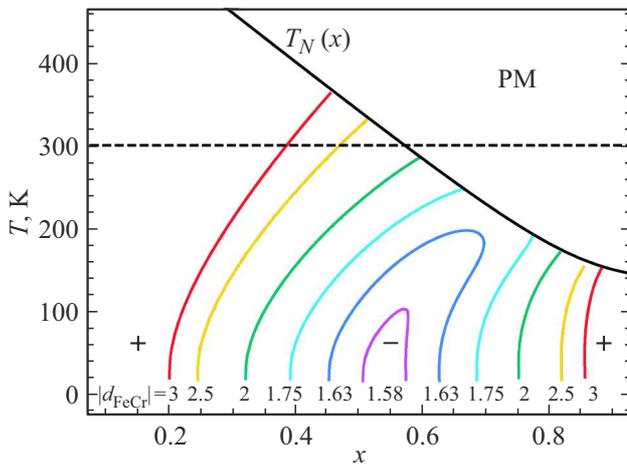
Figure 3. Phase diagram $T - x$ of the areas of magnetization compensation at different values $d_{FeCr} < 0$. The sign „+" indicates the area „of positive" magnetization. Dotted line — room temperature $T = 300$ K.

experimentally discovered transitions for these compositions with a change in the orientation of the weakly ferrimagnetic moment in the a-plane [2] suggests the possible realization of the spatial orientation of the antiferromagnetism vector, that is, the configuration G_{xyz}.

The analysis of the model showed that the magnetization sharply drops with deviation from the parent compositions when the Dzyaloshinskii vector d_{FeCr} for a pair of ions Fe-Cr is directed opposite to the vectors d_{FeFe} and d_{CrCr} (for pairs Fe-Fe and Cr-Cr, respectively), but a region of negative magnetization appears on the phase diagram $T - x$ at $|d_{FeCr}| \geq |d_{FeCr}^{(cr)}|$, where $d_{FeCr}^{(cr)} \approx -1.55$ K, and grows with the growth of $|d_{FeCr}|$ bounded by two lines of compensation points.

Figure 3 shows the phase diagram $T - x$ of a weak ferrimagnet $YFe_{1-x}Cr_xO_3$, where the curve $T_N(x)$ bounds

the region of magnetic ordering, and the curves located below, denote the lines of compensation points, that is, the reversal of the sign of magnetization at different values of the parameter d_{FeCr}. The area between the lines of compensation points is a region of negative magnetization at a certain value of the parameter d_{FeCr}. The system we are considering $YFe_{1-x}Cr_xO_3$ corresponds to two lines, or two areas, of compensation points with $|d_{FeCr}| = 2.5$, where „wide" area is $0.25 \leq x \leq 0.5$ and „narrow" area is close to $x \approx 0.83$.

We would like to note the existence of a fairly large range of parameter values d_{FeCr}, at which the compensation temperature in a weak ferrimagnet $YFe_{1-x}Cr_xO_3$ falls into the practically most important room temperature range of the order of $T = 300$ K, in particular, the compensation temperature reaches room temperature $T = 300$ K in the composition with $x \approx 0.45$ with the parameter $d_{FeCr} = d_{CrFe} = -2.5$ K that we chose.

Unlike $YFeO_3$ and $YCrO_3$, which are weak ferromagnets with a basic magnetic structure of type Γ_4 below the Neel temperature, weak ferrimagnets such as orthoferrites-orthochromites $YFe_{1-x}Cr_xO_3$ demonstrate a complete or partial spin-reorientation of the type $\Gamma_4 - \Gamma_2$ in a wide range of substitution [27]. This unexpected behavior, which is usually typical for orthoferrites with magnetic rare-earth ions (Er, Tm, Dy, ...), is primarily attributable to a strong decrease of the contribution of the DM interaction to magnetic anisotropy. This can be seen when comparing the free energy Φ_{Γ_4} in the phase Γ_4 with the energy Φ_{Γ_2} in the phase Γ_2. The calculations show (see Figure 4) that the first anisotropy constant $k_1 = \frac{1}{2}(\Phi_{\Gamma_2} - \Phi_{\Gamma_4})$ experiences a minimum near the concentration of $x \approx 0.65$, i.e. here the phase Γ_4 is less advantageous in comparison with parent compositions. When taking into account the single-
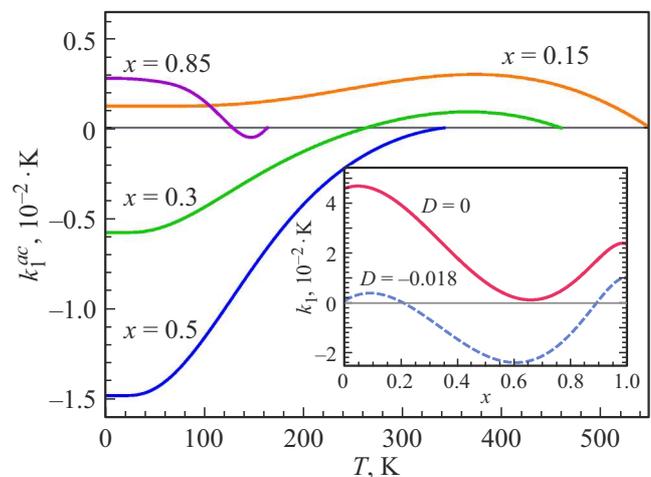
Figure 4. Example of the temperature dependence of the first anisotropy constant k_1 for a-plane at single-ion anisotropy $D = -0.018$ K and at different chromium concentrations x; the inset shows the dependence $k_1(x, T = 0)$.

ion anisotropy $\hat{H}^{(2)}_{SIA}$, the constant k_1 can become negative, which explains the transition to the phase Γ_2.

5. Conclusion

We considered the spin-Hamiltonian of the system $YFe_{1-x}Cr_xO_3$ taking into account the basic isotropic and anisotropic interactions. The average magnitude of the magnetic moments of $3d$-ions and the effective anisotropy constant were calculated within the framework of the molecular field approximation. The existence of two regions of compensation points, „wide" $0.25 \leq x \leq 0.5$ and „narrow" near $x \approx 0.83$, limiting the area of negative magnetization was shown in the model system of $YFe_{1-x}Cr_xO_3$. The compensation temperature reaches room temperature at $x \approx 0.45$ for the system under consideration. The phenomenon of spin reorientation observed for monocrystalline samples in a wide range of concentrations is explained by a sharp decrease of the contribution of antisymmetric exchange to magnetic anisotropy with an increase in deviation from parent compositions and competition with the contribution of single-ion anisotropy of Fe and Cr ions. It was suggested that the spatial orientation of the antiferromagnetism vector (Neel vector) and the G_{xyz} configuration is the reason for the small saturation magnetization observed experimentally for compositions inside or near the negative magnetization region.

Funding

Conflict of interest

The authors declare that they have no conflict of interest.

References

[1] K.P. Belov, A.K. Zvezdin, A.M. Kadomtseva, R.Z. Levitin. Orientatsionniye perekhody v redkozemelnykh magnetikakh. Nauka, M. (1979). 317 s. (in Russian).

[2] A.M. Kadomtseva, A.S. Moskvin, I.G. Bostrem, B.M. Vanklin, N.A. Hafizova. ZhETF **72**, 2286 (1977). (in Russian).

[3] M. Jinhua, Y. Sui, X. Zhang, Y. Su, Kh. Van, Z. Liu, R. Van, Y. Zhu, W. Wang. App. Phys. Lett. **98**, 192510 (2011).

[4] N. Dasari, P. Mandal, A. Sundaresan, N.S. Vidhyadhiraja. Europhys. Lett. **99**, 17008 (2012).

[5] T. Bora, S. Ravi. J. Appl. Phys. **114**, 033906 (2013).

[6] V. Nair, V. Subramanian, P. Santhosh. J. Appl. Phys. **113**, 21 (2013).

[7] F. Pomiro, R.D. Sánchez, G. Cuello, A. Maignan, C. Martin, R.E. Carbonio. Phys. Rev. B **94**, 134402 (2016).

[8] O.V. Billoni, F. Pomiro, S.A. Cannas, C. Martin, A. Maignan, R.E. Carbonio, J. Phys.: Condens. Matter **28**, 476003 (2016).

[9] A.P.G. Rodrigues, M.A. Morales, R.B. Silva, D.R.A.B. Lima, R.L.B.A. Medeiros, J.H. Ara'ujo, D.M.A. Melo. J. Phys. Chem. Solids **141**, 109334 (2020).

[10] R. Salazar-Rodriguez, D. Aliaga Guerra, J.-M. Greneche, K.M. Taddei, N.-R. Checca-Huaman, E.C. Passamani, J.A. Ramos-Guivar. Nanomaterials **12**, *19*, 3516 (2022).

[11] J. Yang, H. Cao, Z. Lu, J. Mo, Y. Zhou, K. Gao, Y. Xia, M. Liu. Phys. Status Solidi B **260**, *7*, 2300145 (2023).

[12] W. Liu, X. Kan, S. Feng et all. J. Mater Sci: Mater Electron. **34**, 793 (2023).

[13] A. Moskvin, E. Vasinovich, A. Shadrin. Magnetochemistry **8**, *4*, 45 (2022).

[14] E.V. Vasinovich, A.S. Moskvin. FTT **65**, *6*, 928 (2023). (in Russian).

[15] A.S. Moskvin. FTT *12*, 3208 (1970). (in Russian).

[16] A.S. Moskvin. E.V. Sinitsyn. FTT **17**, 2495 (1975). (in Russian).

[17] A.S. Moskvin. I.G. Bostrem, FTT **19**, 1616 (1977).

[18] A.S. Moskvin. JMMM **400**, 117 (2016).

[19] A.S. Moskvin. JMMM **463**, 50 (2018).

[20] A. Moskvin. Condens. Matter **4**, *4*, 84 (2019).

[21] A. Moskvin. Magnetochemistry **7**, *8*, 111 (2021).

[22] A.S. Moskvin. ZhETF **159**, 607 (2021). (in Russian).

[23] Mingyu Shang, Chenyang Zhang, Tingsong Zhang, Lin Yuan, Lei Ge, Hongming Yuan, Shouhua Feng. Appl. Phys. Lett. **102**, *6*, 062903 (2013).

[24] R. Salazar-Rodriguez, D. Aliaga Guerra, J.-M. Greneche, K.M. Taddei, N.-R. Checca-Huaman, E.C. Passamani, J.A. Ramos-Guivar. Nanomaterials **12**, *19*, 3516 (2022).

[25] A.S. Moskvin, N.S. Ovanesyan, V.A. Trukhtanov. Hyperfine Interactions **1**, 265 (1975).

[26] A.M. Kadomtseva, V.N. Milov, A.S. Moskvin, M. Pardavi-Horvath. FTT **20**, 817 (1978). (in Russian).

[27] A. Dahmani, M. Taibi, M. Nogues, J. Aride, E. Loudghiri, A. Belayachi. Mater. Chem. Phys. **77**, 912 (2003).

Translated by A.Akhtyamov